Available online at www.sciencedirect.com

ScienceDirect

Energy Procedia 158 (2019) 2567–2579

Energy Procedia

www.elsevier.com/locate/procedia

10th International Conference on Applied Energy (ICAE2018), 22-25 August 2018, Hong Kong, China

Investigation of the flexibility of a residential net-zero energy building (NZEB) integrated with an electric vehicle in Hong Kong

Yuekuan Zhou[a], Sunliang Cao[a,*]

[a] *Renewable Energy Research Group (RERG), Department of Building Services Engineering, Faculty of Construction and Environment, The Hong Kong Polytechnic University, Kowloon, Hong Kong*

Abstract

The flexibility of a net zero energy/emission building (NZEB) in the cooling dominated area is quantitatively investigated in this research. Flexibility sources include the renewable energy, i.e. building integrated photovoltaics (BIPVs) and wind turbine, and thermal energy storages, i.e. air handling unit cooling storage tank (ACST) and domestic hot water tank (DHWT). Parametric analysis has been conducted based on all proposed flexibility indicators with respect to the renewable energy capacity, the volume of both the ACST and the DHWT, and the set point temperature for recharging the DHWT. From our results, to meet the annual energy balance, this NZEB should be equipped with BIPVs and an 8 kW wind turbine, while these BIPVs should be installed on four walls and the roof (totally 306 m^2 BIPVs). Considering the grid feed-in tariff in Hong Kong, the NZEB will get the net annual operational income at 646.3 HK$/$m^2$.a. Flexibility factors indicate the flexibility of the energy storage systems for storing the surplus renewable energy (REe) and fulfilling the building demand. During the charging process, the increase of the REe capacity shows positive impact on flexibility factors of both the ACST and the DHWT. In the case when BIPVs are on four walls, with respect to the increase of the rated wind turbine capacity from 0 to 8 kW, the flexibility factor of the ACST increases from 0.49 to 0.58 during the charging process, whereas it decreases from -0.51 to -0.59 during the discharging process. Meanwhile, the flexibility factor of the DHWT increases from 0.32 to 0.57. Moreover, with respect to the increase of the ACST volume from 0.5 m^3 to 2.5 m^3, the flexibility factor increases from -0.23 to 0.17 considering both the charging and the discharging processes. With respect to the increase of the DHWT volume from 1 m^3 to 3 m^3, the flexibility factor increases from 0.32 to 0.74. With respect to the increase of the set point temperature for recharging the DHWT from 65 ºC to 100 ºC, the flexibility factor increases from 0.32 to 0.82. Moreover, in comparison with the nighttime interaction between the building and the vehicle, the daytime interaction will reduce the reliance on the grid for charging the EV. Moreover, the energy interaction between the building and the vehicle will be enhanced.

Peer-review under responsibility of the scientific committee of ICAE2018 – The 10th International Conference on Applied Energy.

* Corresponding author. Tel.: (+852) 27665837;
E-mail address: sunliang.cao@polyu.edu.hk; caosunliang@msn.com

1876-6102
Peer-review under responsibility of the scientific committee of ICAE2018 – The 10th International Conference on Applied Energy.
10.1016/j.egypro.2019.02.005

Keywords: Renewable energy (REe); Electric vehicle (EV); Building flexibility; Net-zero energy/emission building (NZEB); Recharging

1. INTRODUCTION

Due to the continuous increase of the energy consumption for the economic development, the renewable energy (REe) has attracted increasing interests all over the world. Enhancing the REe penetration into buildings by improving its matching and flexibility is regarded as one of the most significant and effective approaches in reducing the dependence on fossil fuels. The building will thus become the prosumer instead of the traditional consumer. The Hong Kong government and the administrator have encouraged the utilization of the REe with the specific grid feed-in tariff (FiT) scheme [1]. The FiT will be completely dependent on the capacity of REe systems. This FiT scheme will come into force from 1st October 2018, and it will be effective for at least 15 years. However, the renewable energy generation is uneven in the spatial distribution and intermittent in the temporal distribution. To improve the use of the renewable energy with the high matching capability and the high flexibility, energy storages have been widely used to shift the peak and to fill the valley of the building load. Finck et al. [2] proposed the demand flexibility indicators from the perspectives of energy, power and cost to characterize the flexibility in the thermal energy storage. Reynders et al. [3] demonstrated the feasibility, benefits and drawbacks of each quantification methodology of the energy flexibility. Apart from thermal storages, Mcpherson et al. [4] validated the necessity to use the electrical storages for assisting the renewable energy. They explored the market design strategy and the regulation for the electric storage. The intra-day power imbalance of the REe generation can be effectively settled by large-scale EV batteries [5]. They also predicted that, with the development of the car sharing and the vehicle automation technologies, the EV storage can also be essential in improving the utilization efficiency of the renewable energy. Moreover, Tarroja et al. [6] compared the difference for the REe utilization between the vehicle-to-grid energy storage and the stationary energy storage system. From their result, compared to stationary energy storage systems, the V2G-based energy storage has less overall flexibility.

From the available literature, the energy flexibility within storages was mainly studied in heating dominated regions with little attention paid to the cooling dominated region. Moreover, little research was concentrated on investigating the impact of both the thermal storage and the recharging strategy on the energy flexibility. In this study, we conducted the research in the cooling dominated area, Hong Kong, to cover the corresponding scientific gap. Moreover, several energy flexibility indicators are specifically proposed, and others are from the literature but with different physical meanings. The NZEB condition is investigated under the Hong Kong climate condition with the deterministic EV travelling schedule. Finally, we quantitatively investigate the impact of the EV battery size and the V2B interaction period on the energy interaction between the building, the EV and the grid.

Nomenclature

Symbols		*eg*	electric grid
		EVB, a	electric vehicle to building, annual
C	cooling power [kW]	*Forced*	forced
E	flexible energy/energy [kWh/m^2.a]	*imp, a*	annual import
G	power generation [kW]	*MR, a*	mandatory power reduction, annual
GT	greater than	*mandatory, a*	mandatory mode, annual
L	cooling load [kW]	*net, a*	annual net value
Max	maximum	*REV, a*	renewable energy to vehicle, annual
t	time-duration [h]	*surp*	surplus
Greek		*short*	shortage
η	ratio	*travelling, a*	travelling, annual

ρ	positive/negative power (power difference) [kW]	*Abbreviations*	
Subscripts		*ACST*	air handling unit cooling storage tank
Aux	auxiliary heater	*B2V*	building to vehicle
AC	AHU cooling	*CEF*	equivalent CO_2 emission factor
chiller,normal	AHU cooling normal chiller	$CO_{2,eq}/kWh_{end}$	equivalent CO_2 emission per kWh electricity
chiller,recharging	ACST recharging chiller	*DHWT*	domestic hot water tank
cooling	cooling	*FSOC*	fractional state of charging
charging	charging process	*FF*	flexibility factor
discharging	discharging process	*FiT*	grid feed-in tariff
Delayed	delayed	*OEF*	on-site energy fraction
DHW	domestic hot water	*OEM*	on-site energy matching
exp, a	annual export	*REe*	renewable energy
e	electricity	*V2B*	vehicle to building
end	end		

2. METHODS

To characterize the flexibility of the thermal storage and the surplus REe-recharging strategy, several concepts are proposed and defined as follows.

Reference case: the case that provides the basic energy demand without any flexibility sources. This is used only for the comparative study to characterize the flexibility provided by various flexibility sources.

Forced period: the time-duration when the cooling load of the building is lower than the cooling power of the chiller, t_{forced}, [h].

Equation (1) presents the forced period. In contrast to the reference [7], which defines the t_{forced} as that, how long the storage can be completely charged from the completely discharged state. Here, we do not assume the storage to be completely charged. The charging state of the ACST is completely dependent on the surplus renewable energy. Secondly, we do not assume that every initial state of the tank is at the completely discharged state. Therefore, the forced time-duration (t_{forced}) proposed in this study is more realistic and accurate than that in the reference [7].

$$t_{Forced} = \int_0^{t_{end}} GT((C_{chiller,normal} + C_{chiller,recharging} - L_{cooling}), 0) \cdot dt \quad (1)$$

where the $C_{chiller,normal}$ and the $C_{chiller,recharging}$ are the cooling power of the normal chiller and the recharging chiller, respectively, [kW]; $L_{cooling}$ is the cooling load of the building, [kW]; t_{end} is the total time-duration for the whole year, 8760 h; dt is the time step, 0.125 h; *GT* is the function as shown below.

$$GT((C_{chiller,normal} + C_{chiller,recharging} - L_{cooling}),0) = \begin{cases} 1 & \text{when } C_{chiller,normal} + C_{chiller,recharging} > L_{cooling} \\ 0 & \text{when } C_{chiller,normal} + C_{chiller,recharging} < L_{cooling} \end{cases} \quad (2)$$

Delayed period: the time-duration when the cooling load of the building is higher than the power of the chiller, $t_{delayed}$, [h].

Equation (3) presents the delayed period. In contrast to [7], which defines the t_{forced} as that, how long the storage can be completely discharged from the completely charged state. Here, we do not assume the storage to be completely discharged. The discharging state of the ACST is completely dependent on the cooling load. Secondly, we do not assume that every initial state of the tank is at the completely charged state. Therefore, the forced time-duration (t_{forced}) is more realistic than that in [7].

$$t_{Delayed}= \int_0^{t_{end}} GT((L_{cooling}-C_{chiller,normal}), 0)\cdot dt \quad (3)$$

REe surplus period: the time-duration when the REe generation is higher than the total electrical demand, t_{surp}, [h]. Equation (4) presents the REe surplus period.

$$t_{surp} =\int_0^{t_{end}} GT((G_{REe}-L_{electricity}), 0)\cdot dt \quad (4)$$

where the G_{REe} and the $L_{electricity}$ are the power of the on-site renewable energy and the total electric demand, respectively, [kW].

REe shortage period: the time-duration when the REe generation is less than the building total electric demand, t_{short}, [h]. Equation (5) presents the REe shortage period.

$$t_{short} =\int_0^{t_{end}} GT((L_{electricity}-G_{REe}), 0)\cdot dt \quad (5)$$

Forced/delayed power flexibility: the capacity to increase/decrease the power consumption during the flexible period, [kW].

The original power flexibility from the references [2,7] only considers the thermal storages. Here, we define the power flexibility considering both thermal storages and the REe-recharging strategy. Equation (6) and (7) present the forced and the delayed power flexibilities, respectively. The forced power indicates that how much additional cooling power of the chiller can be generated even though the cooling load is met. The larger the forced power is, the more flexible the system will be. The delayed power indicates that how much cooling power of the chiller can be shifted from the time when the cooling load is required. The larger the delayed power is, the more flexible the system will be.

$$\rho_{Forced} =Max(((C_{chiller,normal}+C_{chiller,recharging} - L_{cooling}),0) \quad (6)$$

$$\rho_{Delayed} =Max((L_{cooling} - C_{chiller,normal}),0) \quad (7)$$

Where the ρ_{Forced} is the forced power of both the normal chiller and the recharging chiller, [kW]; $\rho_{Delayed}$ is the delayed power of the normal chiller, [kW]; *Max* is the function as shown below.

$$Max((L_{cooling}-C_{chiller,normal}),0)=\begin{cases} L_{cooling}-C_{chiller,normal} & \text{when } L_{cooling}> C_{chiller,normal} \\ 0 & \text{when } L_{cooling}<C_{chiller,normal} \end{cases} \quad (8)$$

Energy flexibility: the integration of the power flexibility over the corresponding flexible period, [kWh/m^2.a].

Equation (9) and (10) present the forced and the delayed energy flexibilities, respectively. The forced energy indicates that how much additional cooling energy of the chiller can be generated even though the cooling load is met. The larger the forced energy is, the more flexible the system will be. The delayed energy indicates that how much cooling energy of the chiller can be shifted from the time when cooling load is required. The larger the delayed energy is, the more flexible the system will be.

$$E_{Forced} =\int_0^{t_{Forced}} \rho_{Forced}dt/A \quad (9)$$

$$E_{Delayed} =\int_0^{t_{Delayed}} \rho_{Delayed}dt/A \quad (10)$$

$$E_{DHW} =\int_0^{t_{surp}} P_{DHW}dt/A \quad (11)$$

$$E_{Aux}= \int_0^{t_{short}} P_{Aux}dt/A \quad (12)$$

where the E_{DHW} indicates the energy consumption for covering the DHW heating demand from the renewable energy, [kWh/m^2.a]; E_{Aux} indicates the energy consumption of the auxiliary heater for covering the DHW heating demand, [kWh/m^2.a]. P_{DHW} is the power sent to the DHWT from the renewable energy, [kW]; P_{Aux} is the power consumption of the auxiliary electric heater for the DHW heating, [kW]; A is the net floor area of our simulated building, 200 m^2.

Flexibility factors (FF): the capability to shift the energy to the preferable period.

In this study, only the surplus REe-recharging strategy is studied. During the REe surplus period (t_{surp}), the surplus REe is expected to be converted to the forced energy (E_{forced}). During the REe shortage period (t_{short}), the delayed energy ($E_{delayed}$) is expected to be used for shifting the cooling energy of the normal chiller. Therefore, the preferable period refers to both the REe surplus period (t_{surp}) and the REe shortage period (t_{short}).

With respect to the cooling system, the recharging chiller will convert the surplus REe to the cooling energy in the AHU storage tank (ACST). Similarly, the surplus REe can be stored in the domestic hot water tank (DHWT) by an electrical heater. Flexibility indicators of both the cooling and the heating systems are defined by Equations (14)-(17). The flexibility factor shown in Equation (13) is from the reference [8], which was originally proposed for the cost analysis. But here, we define the flexibility factor for investigating the capability of the system in terms of proving the flexible energy.

$$FF=\frac{\int_0^{t_{\text{low price time}}} q_{heating}dt-\int_0^{t_{\text{high price time}}} q_{heating}dt}{\int_0^{t_{\text{low price time}}} q_{heating}dt+\int_0^{t_{\text{high price time}}} q_{heating}dt} \tag{13}$$

$$FF_{charging}=\frac{\int_0^{t_{surp}} \rho_{Forced}dt-\int_0^{t_{short}} \rho_{Forced}dt}{\int_0^{t_{surp}} \rho_{Forced}dt+\int_0^{t_{short}} \rho_{Forced}dt} \tag{14}$$

$$FF_{discharging}=\frac{\int_0^{t_{short}} \rho_{Delayed}dt-\int_0^{t_{surp}} \rho_{Delayed}dt}{\int_0^{t_{short}} \rho_{Delayed}dt+\int_0^{t_{surp}} \rho_{Delayed}dt} \tag{15}$$

$$FF_{AC}=w_1\cdot FF_{charging}+w_2\cdot FF_{discharging} \tag{16}$$

$$FF_{DHW}=\frac{\int_0^{t_{surp}} P_{DHW}dt-\int_0^{t_{short}} P_{Aux}dt}{\int_0^{t_{surp}} P_{DHW}dt+\int_0^{t_{short}} P_{Aux}dt} \tag{17}$$

where w_1 and w_2 are the weighing factors during both the charging and the discharging processes, respectively. In this study, for the simplification, they both have the same value at 0.5.

The $FF_{charging}$ indicates the capability for shifting the forced energy to the REe surplus (t_{surp}) period compared to the REe shortage (t_{short}) period. The $FF_{discharging}$ indicates the capability for shifting the delayed energy to the REe shortage (t_{short}) period compared to the REe surplus (t_{surp}) period. FF_{AC} indicates the capability for shifting the forced energy and the delayed energy to the preferable period during both charging and discharging processes. FF_{DHW} indicates the capability of the surplus REe for the DHW heating compared to the auxiliary heater at the REe shortage (t_{short}) period. All flexibility factors range from -1 to 1. The larger the flexibility factors are, the more flexible the system will be.

To investigate the impact of the EV integration on the energy interaction between the building, the EV and the grid, several indicators are calculated by the following equations.

$$\eta_{REV,a}=\frac{E_{REV,a}}{E_{REV,a}+E_{mandatory,a}} \tag{18}$$

$$\eta_{EVB,a}=\frac{E_{EVB,a}}{E_{EVB,a}+E_{travelling,a}} \tag{19}$$

$$\eta_{MR,a}=\frac{E_{travelling,a}-E_{mandatory,a}}{E_{travelling,a}} \tag{20}$$

where $E_{REV,a}$ is the annual energy to the EV from the renewable energy, [kWh/m^2.a]; $E_{EVB,a}$ is the annual energy to the building from the EV, [kWh/m^2.a]; $E_{mandatory,a}$ is the annual energy from the grid for charging the EV under the mandatory mode, [kWh/m^2.a]; $E_{travelling,a}$ is the annual EV energy demand for the transportation purpose, [kWh/m^2.a]. $\eta_{REV,a}$ indicates the ratio of the annual total energy charged to the EV from the renewable energy, referring to the reference [9]; $\eta_{EVB,a}$ indicates the ratio of the annual total energy charged to the EV battery being used for covering the electric demand of the building; $\eta_{MR,a}$ is the ratio of the annual EV energy demand for the transportation purpose covered by the renewable energy. They all range from 0 to 1. The larger the indicators are, the better the energy interaction between the building, the EV and the grid will be.

3. System configuration and modelling

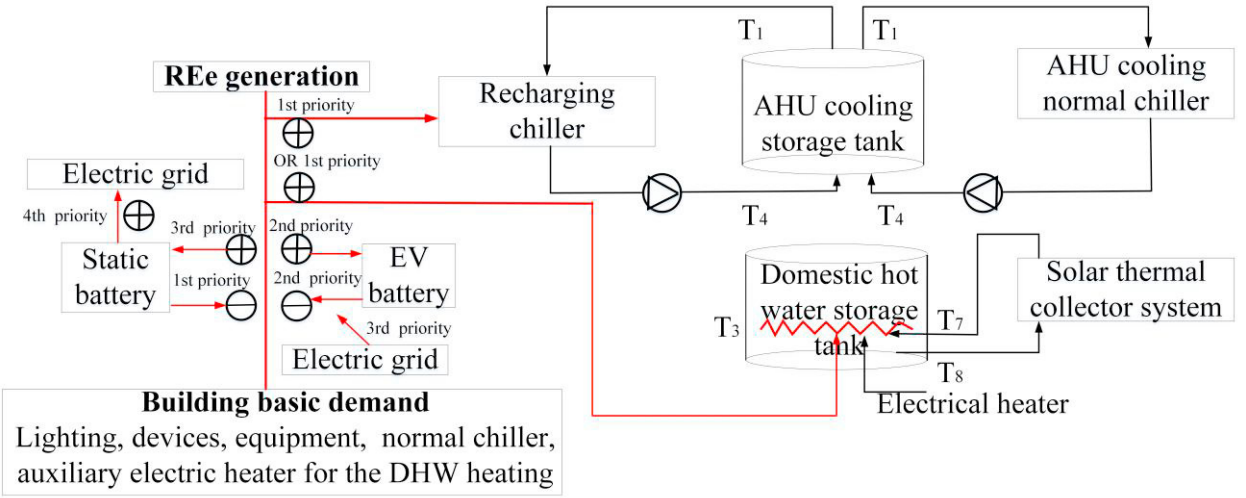

Fig. 1. The brief configuration and the control principle of the system

3.1. Simulation modelling

This research is conducted on the Transient System Simulation Program called TRNSYS 18, which is a dynamic simulation environment for the building energy technology, the HVAC and renewable energy systems. The open source code-based models (Types) make it possible for refining the existing model or developing new models. This enhances the applicability and the practicability of the simulation tool in the building energy simulation.

There are several energy storage systems in our system, including the thermal energy storage systems, such as the AHU cooling storage tank (ACST) and the domestic hot water tank (DHWT), and the electrical energy storage systems. Considering the accuracy and the convergence of each component in our system, the time step of our simulation is selected as 0.125 h. The simulated single-family house is located at New Territory, a suburb in Hong Kong (22.3 ºN, 114.2º E). The heating system is composed of a solar thermal collector system, a DHW tank and an auxiliary electric heater. The water flows through the DHW tank before being heated by the auxiliary electric heater to the required temperature of 60 ºC. The cooling system includes an AHU cooling chiller, an AHU storage tank (ACST) and control pumps. The volume and the height of the DHW storage tank and the AHU cooling storage tank are 1 m^3/1.08 m and 1.5 m^3/1.15 m, respectively. Moreover, one recharging chiller is installed for recharging the REe-ACST with the assumed nominal COP at 2.1. The rated capacity of the normal chiller in our system is around 10 kW, and the rated COP of the normal chiller is 3.6. The on-site surplus REe can be used either for the REe-ACST or the REe-DHWT, depending on the applied REe-recharging strategy. The set point temperature (chilled water temperature leaving from the evaporator) for recharging the REe-ACST is defined by Eq. (21).

$$T_{REe\text{-}ACST}=5\text{-}4\times GT(surplus,0) \quad (21)$$

3.2. System configuration and control

Fig. 1. shows the operational and the control principle of our system. As shown in Fig. 1, when the REe generation is higher than the basic demand, one option is to drive the REe-ACST recharging chiller to convert the surplus REe to the cooling energy in the ACST, resulting in the decrease of the basic demand. Another option is the REe-DHWT recharging strategy, which will reduce the electric consumption of the auxiliary heater for the DHW heating. This also results in the decrease of the basic demand. These two recharging strategies will enhance the forced energy in both tanks. If there is still surplus REe generation left, it will be sent to the EV battery and then to the static battery. Finally, the rest of the surplus REe generation will be exported to the electric grid.

During the period when the REe generation is insufficient to cover the basic demand, the delayed energy in both the ACST and the DHWT will be used to back up the on-site energy shortage. If there is still any shortage when the ACST and the DHWT are completely discharged, the static battery and the EV battery will be subsequently discharged to cover the shortage. In the end, the rest of the on-site energy shortage will be covered by the imported electricity from the electric grid.

4. Results

4.1 Flexibility analysis in the cooling system

Generally, in the case without any cooling storage tanks, the chiller should be operated whenever there is any cooling load. The postponement of the operational time-duration of the chiller is resulting from the use of the storage tank. In that sense, the coupling of a chiller to a storage unit creates a certain degree of the flexibility, and the cooling power/energy of the chiller can be shifted in time. When the operational time-duration of the chiller can be postponed while the energy demand is met by the storage tank, the delayed flexibility is then calculated.

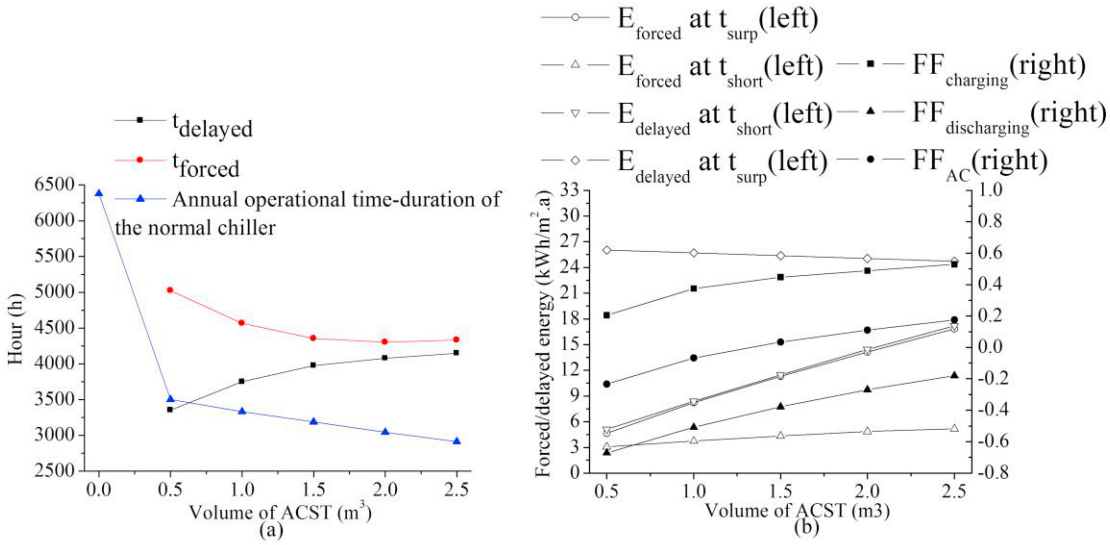

Fig. 2. The impact of the ACST volume on the operational time-duration (a) and the energy flexibility/flexibility factor (b)

Fig. 2 (a) shows the variation of the operational time-duration of the chiller with respect to the increase of the ACST volume. As shown in Fig. 2 (a), the annual operational time-duration of the AHU cooling chiller will be reduced with the equipment of the ACST. The 0.5 m^3 ACST can reduce the annual operational time-duration of the normal chiller from 6379 h to 3502 h by 45.1%. The annual operational time-duration can be further reduced to 2912 h with respect to the increase of the ACST volume from 0.5 m^3 to 2.5 m^3. This is because that the ACST with the larger volume can store more renewable energy, and thus it can cover the AHU cooling load with the decreased operational time-duration of the normal chiller. Furthermore, with respect to the increase of the ACST volume from 0.5 m^3 to 2.5 m^3, the forced time-duration decreases from 5024 to 4332 h, whereas the delayed time-duration increases from 3352 to 4149 h. It

should also be noted that the slope of both curves decreases with respect to the increase of the ACST volume. This is because that when the ACST volume is not sufficient for storing the surplus renewable energy, the capability of the ACST for storing the surplus REe is limited by its volume. However, the capability of the ACST for storing the surplus REe is limited by the REe generation when its volume exceeds the maximum volume for storing the surplus renewable energy. The saturation in both curves results from the limited amount of the renewable energy generation. Moreover, when the ACST volume exceeds 1.5 m^3, the increasing ratio of the delayed time-duration curve starts to slow down more noticeably. As a result, the ACST volume of 1.5 m^3 is more competitive than others in terms of reducing the forced time-duration and enhancing the delayed time-duration. For instance, in comparison with the ACST volume of 0.5 m^3, the delayed time-duration will be increased from 3352 h to 3974 h by 18.6%, and the forced time-duration will be decreased from 5024 h to 4353 h by 13.4%. With respect to the further increase of the ACST volume from 1.5 m^3 to 2.5 m^3, the delayed time-duration will be increased only from 3974 h to 4149 h by 4.4%, and the forced time-duration will be decreased only from 4353 h to 4332 h by 0.5%.

The effect of the ACST volume on the forced/delayed energy is shown in Fig. 2 (b). As shown in Fig. 2 (b), with respect to the increase of the ACST volume from 0.5 m^3 to 2.5 m^3, the delayed energy at the REe shortage period (t_{short}) increases from 5.1 to 17.2 kWh/m^2.a. This indicates that the capability of the ACST is improved in terms of covering the building cooling load by itself. Meanwhile, with respect to the increase of the ACST volume from 0.5 m^3 to 2.5 m^3, the forced energy at the REe shortage period (t_{short}) increases a bit from 3.1 to 5.2 kWh/m^2.a, whereas the delayed energy at the REe surplus period (t_{surp}) decreases from 26 to 24.7 kWh/m^2.a. Overall, several conclusions can be reached. Firstly, by adopting the REe-ACST recharging strategy, the forced energy at the REe shortage period (t_{short}) is far lower than the delayed energy at the REe surplus period (t_{surp}). This tendency will be more obvious with respect to the increase of the ACST volume. Secondly, with respect to the increase of the ACST volume, the delayed energy at the REe shortage period (t_{short}) will be increased, whereas the delayed energy at the REe surplus period (t_{surp}) will be reduced. Therefore, increasing the ACST volume is technically feasible for enhancing the energy flexibility during both the charging and the discharging processes.

Moreover, Fig. 2 (b) also shows the evolution of flexibility factors during both the charging and the discharging processes. With respect to the increase of the ACST volume from 0.5 m^3 to 2.5 m^3, the flexibility factor increases from -0.23 to 0.17. As shown in Fig. 2 (b), when the ACST volume is 1.5 m^3, the increasing ratio of the $FF_{charging}$ curve starts to slow down. The reason is similar to the delayed time-duration ($t_{delayed}$) as explained above. The reason of the negative $FF_{discharging}$ is that, due to the REe-ACST recharging strategy, the delayed energy at the REe surplus period (t_{surp}) is far higher than the delayed energy at the REe shortage period (t_{short}). As a result, the critical volume of the ACST is 1.5 m^3 considering both the increasing magnitude of the FF_{AC} and the available space for installing the ACST in the residential building.

4.2 Flexibility analysis in the DHWT

The effect of the REe-DHWT recharging strategy on the energy flexibility and flexibility factors is investigated in this section. Parametric study has been conducted using the control variable method with respect to the DHWT volume and the set point temperature for recharging the DHWT. More specifically, when we conduct the DHWT volume analysis, the set point temperature for recharging the DHWT is kept at 65 ºC. When we investigate the impact of the set point temperature on the capability of the REe for recharging the DHWT, the DHWT volume is kept at 1 m^3.

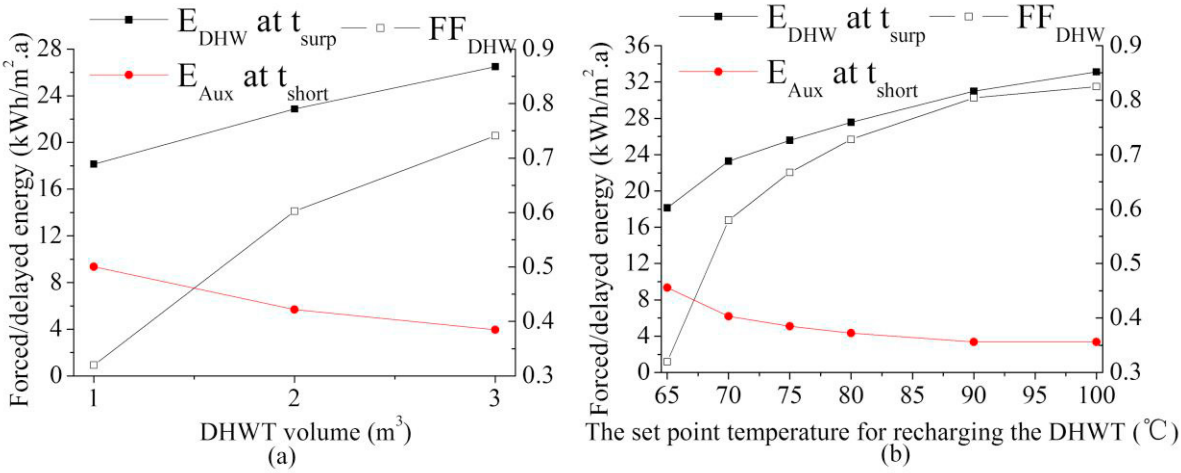

Fig. 3. The impact of the DHWT volume (a) and the set point temperature for recharging the DHWT (b) on the E_{DHW}, the E_{Aux} and the FF_{DHW}

The effect of the DHWT volume on the E_{DHW} and the E_{Aux} is shown in Fig. 3 (a). As shown in Fig. 3 (a), with respect to the increase of the DHWT volume, the E_{DHW} at the REe surplus period (t_{surp}) increases linearly while the E_{Aux} at the REe shortage period (t_{short}) decreases. This is because that the capability in storing the surplus REe is enhanced in the DHWT with a larger volume. Correspondingly, with respect to the increase of the DHWT volume from 1 m^3 to 3 m^3, the flexibility factor increases from 0.32 to 0.74. The impact of the set point temperature for recharging the DHWT on the forced/delayed energy and the FF_{DHW} is illustrated in Fig. 3 (b). With respect to the increase of the set point temperature for recharging the DHWT, the E_{DHW} at the REe surplus period (t_{surp}) increases, while the E_{Aux} at the REe shortage period (t_{short}) decreases. Moreover, the increasing ratio of the E_{DHW} curve starts to slow down more noticeably when the set point temperature for recharging the DHWT is at 90 ºC. Correspondingly, with respect to the increase of the set point temperature for recharging the DHWT from 65 ºC to 100 ºC, the flexibility factor increases from 0.32 to 0.82. Overall, it can be concluded that the flexibility utilization can be improved by either increasing the DHWT volume or improving the set point temperature for recharging the DHWT.

4. 3. NZEB condition discussion

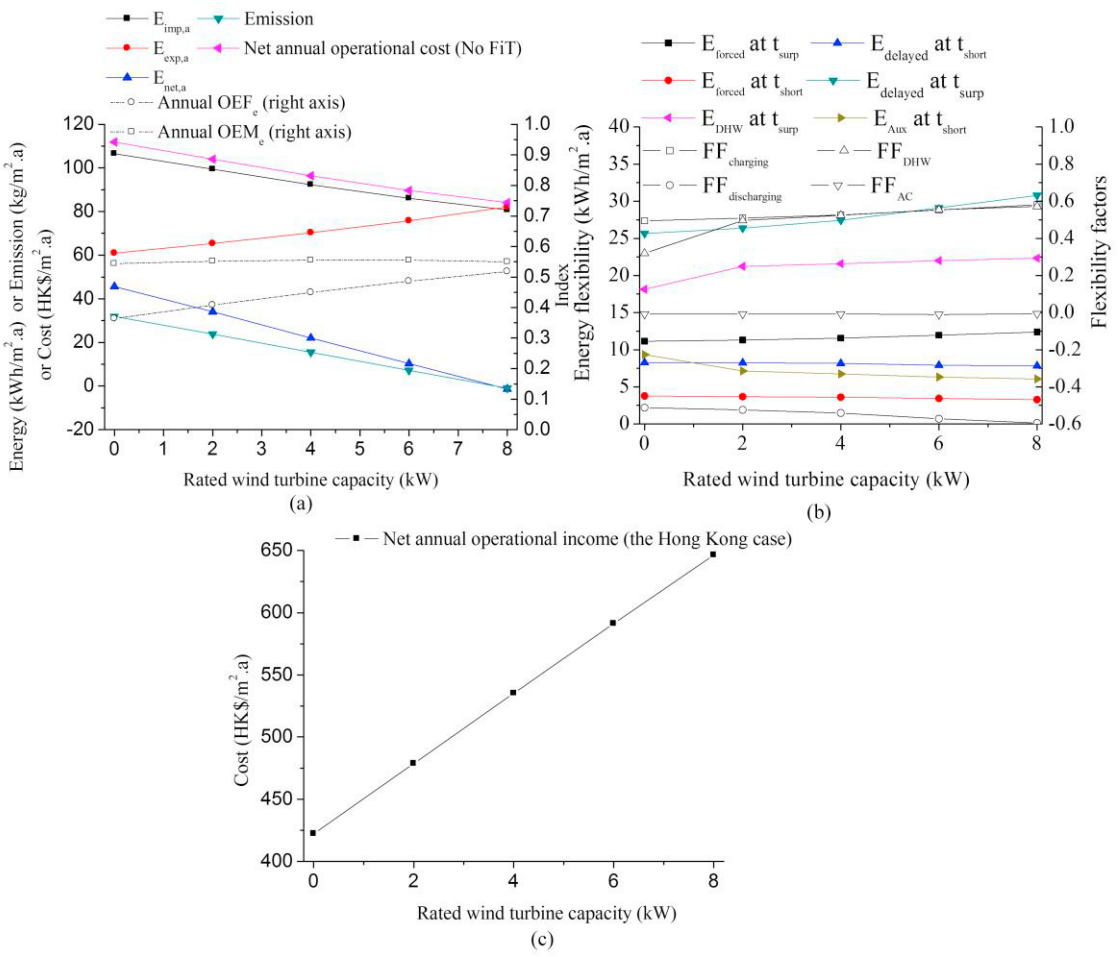

Fig. 4. The effect of the rated wind turbine capacity on the annual equivalent CO_2 emission, the net annual operational cost, the annual matching capability (a), the flexibility factors (b) and the annual operational income under the FiT in Hong Kong (c) when BIPVs are on four walls and the roof (Note: the reference case shows the $E_{imp,a}$, the $E_{exp,a}$, the annual equivalent CO_2 emission and the net annual operational cost of 193.6 kWh/m^2.a, 0 kWh/m^2.a, 135.5 kg/m^2.a and 209.3 HK$/m^2.a, respectively)

The simulation results of the hybrid renewable system are demonstrated and illustrated in Fig. 4. As shown in Fig. 4 (a). A reference case is simulated for the comparative analysis. All geometrical and operational parameters are the same as the studied system, except for the lack of the on-site renewable system and REe-recharging strategies. In comparison with the reference case, the $E_{imp,a}$, the $E_{exp,a}$, the annual equivalent CO_2 emission and the net annual operational cost are decreased by different levels, depending on the capacity of the renewable system. Moreover, on the one hand, when there is no grid feed-in tariff (FiT) for exporting the REe to the electric grid, the net annual operational cost shows a similar trend as that of the $E_{imp,a}$ curve. On the other hand, when there is a feed-in tariff (FiT) of 4 HK$/kWh in Hong Kong [1], the situation will be changed as follows. With respect to the increase of the rated capacity of the wind turbine from 0 to 8 kW, the net annual operational income can be increased from 422.2 to 646.3 HK$/m^2.a by 53.1%. The annual equivalent CO_2 emission shows a similar trend as that of the $E_{net,a}$ curve. This is because that, the CEF_{eg} is a constant value at 0.7 kg $CO_{2,eq}$/kWh$_{end}$. Furthermore, the annual OEF_e increases continuously, which is characterized by the increase of the OEF_e from 0.36 to 0.52 and the decrease of the $E_{imp,a}$ from 106.6 to 80.7 kWh/m^2.a. It indicates that the ratio of the building demand covered

by the REe generation is increased from 36% to 52%. However, the annual OEM_e keeps almost constant at 0.55. This is because that, although the total REe generation increases, the $E_{exp,a}$ increases with a comparable magnitude with the REe generation due to the REe-recharging strategy. Specifically, with respect to the increase of the rated capacity of the wind turbine from 0 to 8 kW, the $E_{exp,a}$ increases from 60.9 to 82.2 kWh/m^2.a by 35%, and the REe generation increases from 133.5 to 182.6 kWh/m^2.a by 36.8%. As a result, with respect to the increase of the rated capacity of the wind turbine from 0 to 8 kW, the $E_{net,a}$ decreases from 45.7 kWh/m^2.a to -1.5 kWh/m^2.a. It indicates that the net-zero energy/emission building (NZEB) can be realized. Correspondingly, the annual OEF_e, the annual OEM_e, the net annual operational income and the annual equivalent CO_2 emission are 0.52, 0.55, 646.3 HK$/m^2.a and -1.1 kg/m^2.a, respectively. This indicates that flexibility sources can improve the annual matching capability and the net annual operational income. Moreover, the annual equivalent CO_2 emission can be decreased by the flexibility sources as well.

Moreover, the impact of the wind turbine capacity on the energy flexibility and flexibility factors is demonstrated in Fig. 4 (b). As shown in Fig. 4 (b), with respect to the increase of the rated wind turbine capacity from 0 to 8 kW, the E_{forced} at the REe surplus period (t_{surp}) increases from 11.1 to 12.4 kWh/m^2.a, whereas the E_{forced} at the REe shortage period (t_{short}) decreases from 3.8 to 3.3 kWh/m^2.a. As a result, the $FF_{charging}$ increases from 0.49 to 0.58, indicating that, compared to the REe shortage (t_{short}) period, the capability of the system is enhanced for shifting the forced energy to the REe surplus (t_{surp}) period. This is because that more forced energy can be generated with respect to the increase of the capacity of the renewable energy. Meanwhile, the $E_{delayed}$ at the REe shortage period (t_{short}) decreases from 8.3 to 7.8 kWh/m^2.a, whereas the $E_{delayed}$ at the REe surplus period (t_{surp}) increases from 25.6 to 30.8 kWh/m^2.a. As a result, the $FF_{discharging}$ decreases from -0.51 to -0.6, indicating that, compared to the REe surplus (t_{surp}) period, the capability is weakened for shifting the delayed energy to the REe shortage (t_{short}) period. This is because that, with respect to the increase of the capacity of the renewable energy, more $E_{delayed}$ will be generated during the REe surplus period (t_{surp}). Moreover, the increase of the REe capacity has little impact on the FF_{AC} as it almost keeps constant at -0.01. This is because that FF_{AC} is dependent on both the $FF_{charging}$ and the $FF_{discharging}$. The increasing magnitude of the $FF_{charging}$ and the decreasing magnitude of the $FF_{discharging}$, will result in the constant value of the FF_{AC}. When there is only the REe-DHWT recharging strategy, the E_{DHW} at the REe surplus period (t_{surp}) increases from 18.1 to 22.3 kWh/m^2.a, whereas the E_{Aux} at the REe shortage period (t_{short}) decreases from 9.3 to 6.1 kWh/m^2.a. As a result, the FF_{DHW} increases from 0.32 to 0.57. This indicates that, compared to the REe shortage (t_{short}) period, the capability of the surplus REe is enhanced in terms of heating the DHW during the REe surplus period (t_{surp}).

4.4. EV discussion in NZEB condition

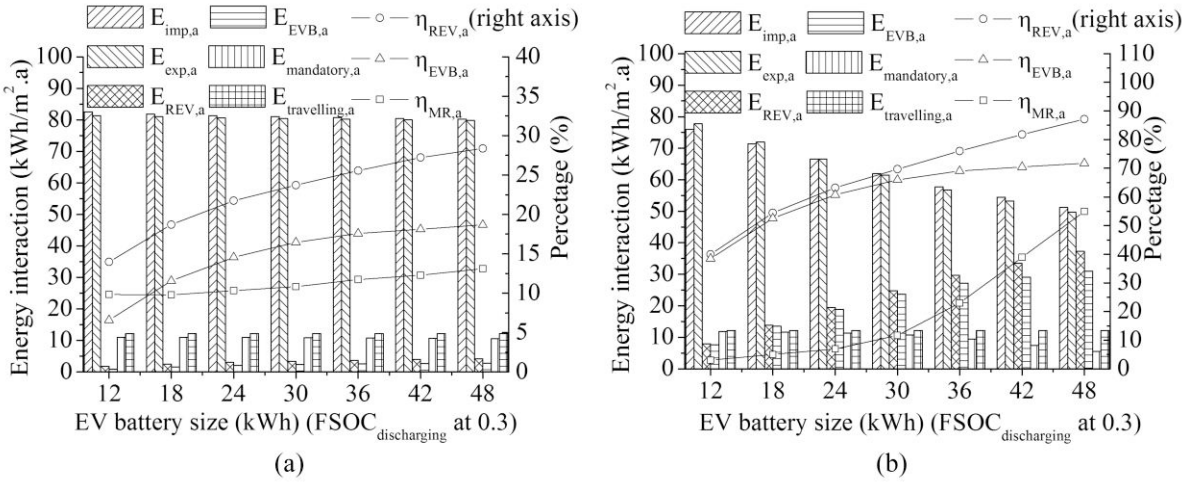

Fig. 5. The impact of the EV battery size on the energy interaction between the building, the grid and the EV, in the NZEB equipped with BIPVs on four walls: (a) the scenario for the EV parking at home at night-time; (b) the scenario for the EV parking at home at daytime

4.4.1. Night-time interaction

In this section, we have investigated the impact of the EV battery size on the grid interaction and the energy interaction between the building, the grid and the EV. The daily travelling distance of the EV is 31.2 km, which is equivalent to an annual energy demand for the transportation purpose ($E_{travelling,a}$) of 12.2 kWh/m^2.a. The EV is parked at home from 18:00 PM to 6:00 AM during the night. Fig. 5 (a) shows the simulation results when the NZEB is equipped with the BIPVs on four walls and the roof. As shown in Fig. 5 (a), the energy interaction between the building, the grid and the EV is enhanced with respect to the increase of the EV battery size. This is indicated by the increment of the $E_{REV,a}$ and the $E_{EVB,a}$. Specifically, with respect to the increase of the EV battery size from 12 kWh to 48 kWh, the $E_{REV,a}$ is increased from 1.8 to 4.2 kWh/m^2.a, and the $E_{EVB,a}$ is increased from 0.9 to 2.8 kWh/m^2.a. Meanwhile, the contribution of the REe to the energy demand for the transportation purpose can be improved as the $\eta_{REV,a}$ increases from 14% to 28.4%. This indicates that the ratio of the annual total energy charged to the EV from the REe can be increased from 14% to 28.4% with respect to the increase of the EV battery size from 12 kWh to 48 kWh. Meanwhile, the $\eta_{EVB,a}$ increases from 6.6% to 18.7%. This indicates that the ratio of the annual total energy charged to the EV battery for covering the building demand can be increased from 6.6% to 18.7%. It should be noted that the $\eta_{MR,a}$ increases from 9.8% to 13.1% with respect to the increase of the EV battery size from 12 kWh to 48 kWh. This indicates the high reliance on the grid for charging the EV and the low ratio of the annual energy demand for the transportation purpose covered by the renewable energy. The potential reasons are described as follows. Firstly, the time-duration for the B2V and the V2B interactions is strictly limited on the night-time. There is no on-site REe generation at night due to the lack of the solar radiation. Secondly, the set value of the $FSOC_{discharging}$ for the V2B interaction is 0.3. This allows the continuous discharging of the EV battery energy until its FSOC reaches 0.3, whereas the shortage of the annual energy demand for the transportation purpose (the FSOC higher than 0.6) is covered by the grid.

4.4.2. Daytime interaction

Fig. 5 (b) shows the energy interaction between the building, the EV and the grid when the NZEB is equipped with BIPVs on four walls and the roof. As shown in Fig. 5 (b), with respect to the increase of the EV battery size from 12 kWh to 48 kWh, the $E_{imp,a}$ is reduced from 76 kWh/m^2.a to 51.2 kWh/m^2.a by 32.6%, and the $E_{exp,a}$ is reduced from 77.8 kWh/m^2.a to 49.7 kWh/m^2.a by 36.1%, respectively. Meanwhile, the energy interaction between the building and the EV can be enhanced, which is indicated by the increase of both the $E_{REV,a}$ and the $E_{EVB,a}$. The former rises from 7.9 kWh/m^2.a to 37.3 kWh/m^2.a, and the latter rises from 7.6 kWh/m^2.a to 31 kWh/m^2.a. Moreover, in comparison with the night-time interaction when there is a 48 kWh EV battery, when the interaction period is at the daytime, the $E_{REV,a}$ increases from 4.2 to 37.3 kWh/m^2.a and the $E_{EVB,a}$ increases from 2.8 to 31 kWh/m^2.a. Moreover, with respect to the increase of the EV battery size from 12 kWh to 48 kWh, the $\eta_{REV,a}$ increases from 40% to 87.2%. This indicates that the ratio of the annual total energy charged to the EV from the REe can be increased from 40% to 87.2%. The $\eta_{EVB,a}$ increases from 38.5% to 71.7%, indicating that the ratio of the annual total energy charged to the EV battery for covering the building demand can be increased from 38.5% to 71.7%. Moreover, the dependence on the grid for the transportation purpose is reduced with respect to the increase of the EV battery size from 12 to 48 kWh. This is indicated by the drop of the $E_{mandatory,a}$ from 11.8 kWh/m^2.a to 5.5 kWh/m^2.a. Correspondingly, the $\eta_{MR,a}$ increases from 3% to 55%. It indicates that the ratio of the annual energy demand for the transportation purpose covered by the renewable energy can be increased from 3% to 55%.

5. Conclusions

In this research, the energy flexibility of the thermal energy storage has been quantitatively characterized. Flexibility factors indicate the flexibility of the energy storage systems for storing the surplus renewable energy (REe) and fulfilling the building demand. Several conclusions can be drawn as follows. Firstly, to meet the energy balance of the NZEB integrated with an EV, the NZEB should be equipped with BIPVs and an 8 kW wind turbine, and these

BIPVs include the 198 m^2 vertical BIPVs on four walls and the 108 m^2 BIPVs on the roof with a tilted angle at 20º. Considering the grid feed-in tariff in Hong Kong, the NZEB will get the net annual operational income at 646.3 HK\$/m^2.a. Secondly, several approaches are validated to be technically feasible in terms of improving the flexibility factors. These approaches include: the REe-ACST and the REe-DHWT recharging strategies, the increase of the volume of both the DHWT and the ACST, an increase of the set point temperature for recharging the DHWT and the increase of the renewable energy capacity. During the charging process, with respect to the increase of the wind turbine capacity from 0 to 8 kW, the $FF_{charging}$ increases from 0.49 to 0.58, and the FF_{DHW} increases from 0.32 to 0.57. The former indicates that the capability of the system is enhanced for shifting the forced energy to the REe surplus (t_{surp}) period compared to the REe shortage (t_{short}) period, and the latter indicates that the capability of the system is enhanced for the DHW heating via the surplus renewable energy compared to the auxiliary heater at the REe shortage (t_{short}) period. However, the $FF_{discharging}$ decreases from -0.51 to -0.59, indicating that the capability is weakened for shifting the delayed energy to the REe shortage (t_{short}) period compared to the REe surplus (t_{surp}) period. Moreover, all flexibility factors will be positively enhanced with respect to the increase of the set point temperature for recharging the DHWT as well as the increase of the ACST and the DHWT volumes. Thirdly, in comparison with the energy interaction between the EV and the building at night, the daytime interaction will increase the energy interaction between the building and the EV, and decrease the grid reliance for charging the EV. In comparison with the nighttime interaction with a 48 kWh EV battery, when the interaction period of the EV and the building is at daytime, the $E_{REV,a}$ increases from 4.2 to 37.3 kWh/m^2.a, and the $E_{EVB,a}$ increases from 2.8 to 31 kWh/m^2.a. Moreover, with respect to the increase of the EV battery size from 12 to 48 kWh, the $E_{mandatory,a}$ decreases from 11.8 to 5.5 kWh/m^2.a. Regarding the energy sharing between the building, the EV and the grid, 87.2% of the annual total energy charged to the EV is from the renewable energy. Meanwhile, 71.7% of the annual total energy charged to the EV can be used for covering the building demand, and 55% of annual energy demand for the travelling purpose can be covered by the renewable energy.

Acknowledgements

This research is supported by the project “The Investigation of the Multi-objective Optimal Zero-energy Buildings with High Energy Flexibilities in Hong Kong” in the Hong Kong Polytechnic University.

References

[1] Feed-in Tariff Scheme and Renewable Energy Certificate, https://www.clpgroup.com/en/Media-Resources/site/Current%20Releases%20Documents/20180423/20180423_Factsheet_FiT_RE%20Cert_en.pdf.

[2] C. Finck, R. Li, R. Kramer, W. Zeiler. Quantifying demand flexibility of power-to-heat and thermal energy storage in the control of building heating systems, Applied Energy, 209 (2017), pp. 409-425.

[3] G. Reynders, R.A. Lopes, A. Marszal-Pomianowska, D. Aelenei, J. Martins, D. Saelens. Energy Flexible Buildings: An evaluation of definitions and quantification methodologies applied to thermal storage. Energy & Buildings, 166 (2018), pp. 372-390.

[4] M. Mcpherson, S. Tahseen. Deploying storage assets to facilitate variable renewable energy integration: the impacts of grid flexibility, renewable penetration, and market structure. Energy, 145 (2018), pp. 856-870.

[5] J. Liu, Z. Hu, B. David, Y. Zhao, Z. Wang, The future of energy storage shaped by electric vehicles: A perspective from China, Energy, 145(2018), pp. 249-257.

[6] B. Tarroja, L. Zhang, V. Wifvat, B. Shaffer, S. Samuelsen. Assessing the stationary energy storage equivalency of vehicle-to-grid charging battery electric vehicles. Energy, 106(2016), pp. 673-690.

[7] S. Stinner, K. Huchtemann, D. Müller. Quantifying the operational flexibility of building energy systems with thermal energy storages. Applied Energy, 181(2016), pp. 140-154.

[8] J.L. Dréau, P. Heiselberg. Energy flexibility of residential buildings using short term heat storage in the thermal mass. Energy, 111(2016), pp. 991-1002.

[9] S. Cao. Comparison of the energy and environmental impact by integrating a H_2, vehicle and an electric vehicle into a zero-energy building. Energy Conversion and Management, 123(2016), pp.153-173.